

# Facile synthesis of highly biocompatible folic acid-functionalized SiO<sub>2</sub> encapsulated rare-earth metal complexes nanoparticles and its application on targeted metal-based complex delivery

Xiuling Xu, Fan Hu and Qi Shuai\*

*Shaanxi Key Laboratory of Natural Products & Chemical Biology, College of Chemistry & Pharmacy, Northwest A&F University, Yangling, Shaanxi 712100, People's Republic of China.*

## Fluorescence microscopy images

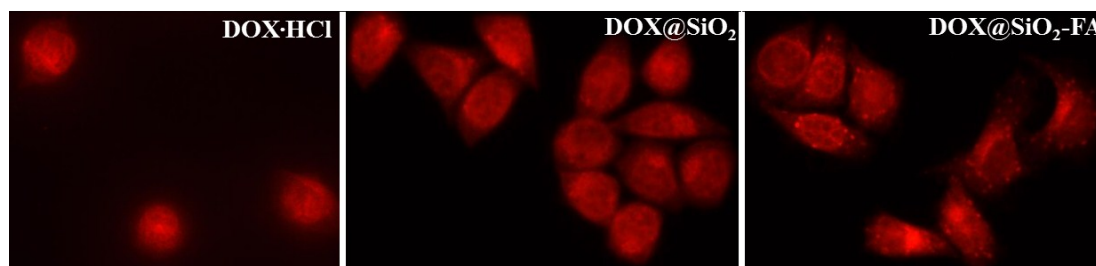


Fig. S1 Fluorescence microscopy images of HepG2 cells incubated with (a) free DOX·HCl, (b) DOX@SiO<sub>2</sub>, (c) DOX@SiO<sub>2</sub>-FA at 37 °C for 4 h (DOX concentration 10 μg mL<sup>-1</sup>).

It was difficult to imaging due to the weak fluorescent of the RC<sub>2</sub>. To simulate this procedure of nanoparticles distribution, we choose DOX·HCl with strong fluorescent to replace the complexes (RC<sub>2</sub>). The synthesis of DOX@SiO<sub>2</sub>-FA was as same as RC<sub>2</sub>@SiO<sub>2</sub>-FA. The results show that free DOX·HCl is transported into cells via diffusion and primarily accumulated in the nuclei of the HepG2 cells where it can lead to cell death by interrupting DNA replication. DOX·HCl delivered via the DOX@SiO<sub>2</sub> was localized in both cytosol and nuclei of the HepG2 cells because it was taken up by the cells through a non-specific endocytosis mechanism and the DOX·HCl released from DOX@SiO<sub>2</sub> could be transported into cells via diffusion and accumulated in the nuclei. In contrast, DOX·HCl delivered via the DOX@SiO<sub>2</sub>-FA was mainly localized in cytosol and dot-shaped fluorescence was observed within cytoplasm, and was considered to be SiO<sub>2</sub> spheres trapped in the endocytic vesicles. Thus, by analyzing the above results, we can prove that the Si-nanoparticles containing rare-earth metals are really delivered into the cells.

## The stability test for nanoparticles

In order to test the stability of nanoparticles, the same concentration of RC<sub>2</sub>@SiO<sub>2</sub> and RC<sub>2</sub>@SiO<sub>2</sub>-FA in the PBS (pH=7.4) for six days, from the picture, we can see in the first five days, RC<sub>2</sub>@SiO<sub>2</sub> and RC<sub>2</sub>@SiO<sub>2</sub>-FA were stable enough without precipitation. But from the sixth day, the RC<sub>2</sub>@SiO<sub>2</sub> began to precipitate, while the RC<sub>2</sub>@SiO<sub>2</sub>-FA is still stable, so that the RC<sub>2</sub>@SiO<sub>2</sub>-FA is sufficiently stable.

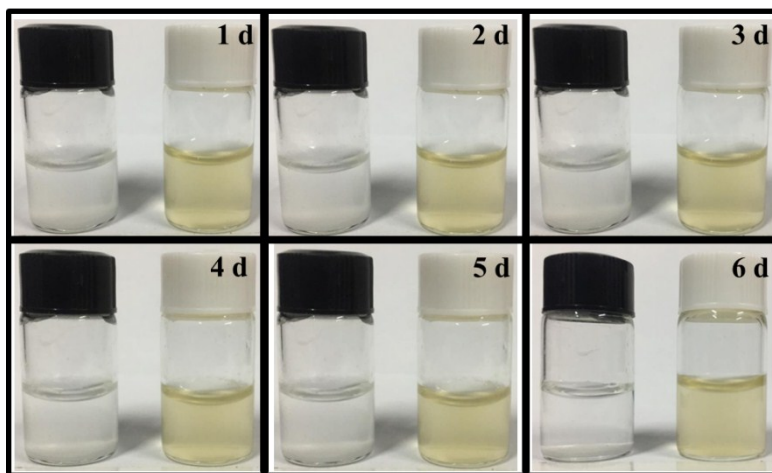


Fig. S2 The stability of the two kinds of nanoparticles(left:  $RC_2@SiO_2$ ; right:  $RC_2@SiO_2-FA$ ).

### In vitro drug release

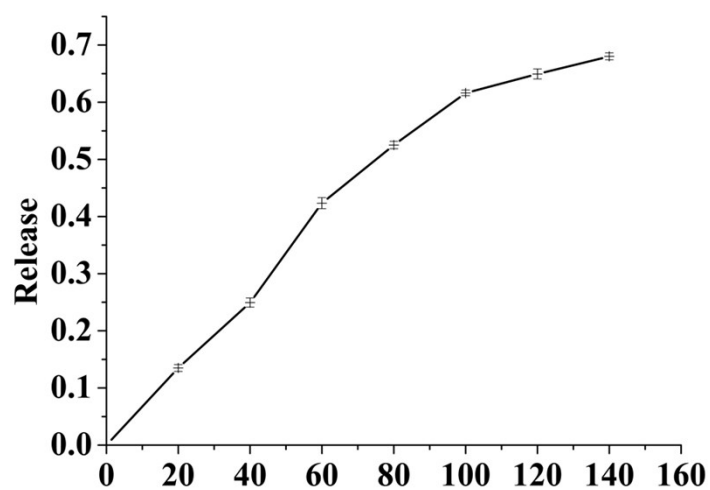


Fig. S3The release curve of  $RC_2@SiO_2-FA$ . The error bars in the graph represent standard deviations (n=3).

### In vitro cytotoxicity studies

The drug release behavior of the nanoparticles was evaluated at 37 °C in PBS (pH=7.4). Nanoparticles which showed a slow release of  $RC_2$  from  $RC_2@SiO_2-FA$ . As showed in Fig S3, about 13.5% of  $RC_2$  was released in the first 20 h and roughly 61.63% released within 100 h. After that, the release becomes slow, the release rate up to 68.03% after 140 hours.

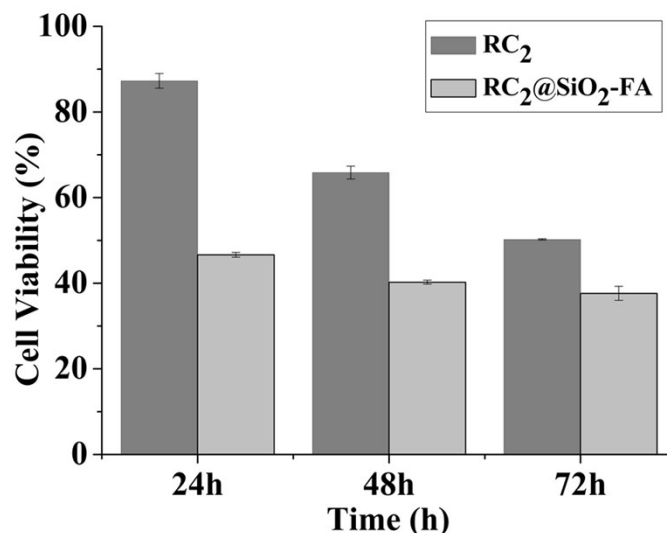


Fig. S4 Cell viability of HepG2 cells treated with RC<sub>2</sub>@SiO<sub>2</sub>-FA and free RC<sub>2</sub> after 24 h, 48 h and 72 h. Data represent mean  $\pm$  SD (n=5). Cell viability was evaluated after incubation with 100  $\mu$ g/mL of free RC<sub>2</sub> and RC<sub>2</sub>@SiO<sub>2</sub>-FA containing a corresponding RC<sub>2</sub> content for 24 h, 48 h and 72 h. After 24 h incubation, a comparison was made between RC<sub>2</sub>@SiO<sub>2</sub>-FA and free RC<sub>2</sub> at equivalent concentration. Fig S4 showed the difference was the cytotoxicity of free RC<sub>2</sub> is inferior to RC<sub>2</sub>@SiO<sub>2</sub>-FA at equal concentrations. This may be attributed to the different intracellular uptake rate of free RC<sub>2</sub> (the passive diffusion mechanism) and nanoparticles (endocytosis, EPR effect). After 48 h and 72 h incubation at 100  $\mu$ g/mL concentration of free RC<sub>2</sub>, the cytotoxicity of free RC<sub>2</sub> had an obvious raise, which based on the fact that more amounts of free RC<sub>2</sub> would transported into cells.

**Table 2. Selected bond lengths ( $\text{\AA}$ ) and angles ( $^\circ$ ) for 1-5**

1			
Er(1)-O(8)A	2.255(7)	Er(1)-O(2W)	2.400(7)
Er(1)-O(4)	2.283(7)	Er(1)-O(1)	2.428(7)
Er(1)-O(7)	2.343(7)	Er(1)-O(2)	2.443(8)
Er(1)-O(1W)	2.366(7)	Er(1)-O(3W)	2.445(6)
O(8)A-Er(1)-O(4)	146.8(3)	O(8)A-Er(1)-O(1)	80.0(3)
O(8)A-Er(1)-O(7)	103.0(2)	O(4)-Er(1)-O(1)	76.4(2)
O(4)-Er(1)-O(7)	85.3(2)	O(7)-Er(1)-O(1)	147.4(2)
O(8)A-Er(1)-O(1W)	139.6(2)	O(1W)-Er(1)-O(1)	116.0(2)
O(4)-Er(1)-O(1W)	72.8(2)	O(2W)-Er(1)-O(1)	75.0(2)
O(7)-Er(1)-O(1W)	83.0(2)	O(8)A-Er(1)-O(2)	83.7(3)
O(8)A-Er(1)-O(2W)	73.2(3)	O(4)-Er(1)-O(2)	100.2(3)
O(4)-Er(1)-O(2W)	78.2(2)	O(7)-Er(1)-O(2)	158.7(3)
O(7)-Er(1)-O(2W)	75.0(2)	O(1W)-Er(1)-O(2)	79.2(3)
O(1W)-Er(1)-O(2W)	144.7(2)	O(2W)-Er(1)-O(2)	126.2(3)
O(1)-Er(1)-O(2)	53.2(2)	O(1W)-Er(1)-O(3W)	68.9(2)
O(8)A-Er(1)-O(3W)	72.6(3)	O(2W)-Er(1)-O(3W)	132.2(2)
O(4)-Er(1)-O(3W)	140.6(2)	O(1)-Er(1)-O(3W)	129.2(2)
O(7)-Er(1)-O(3W)	81.4(3)	O(2)-Er(1)-O(3W)	81.4(2)
2			
Ho(1)-O(8)A	2.245(7)	Ho(1)-O(2W)	2.386(7)
Ho(1)-O(4)	2.272(7)	Ho(1)-O(2)	2.416(7)
Ho(1)-O(1W)	2.348(7)	Ho(1)-O(1)	2.418(8)
Ho(1)-O(7)	2.355(7)	Ho(1)-O(3W)	2.456(7)

O(8)A-Ho(1)-O(4)	146.8(3)	O(8)A-Ho(1)-O(2)	85.4(3)
O(8)A-Ho(1)-O(1W)	140.4(3)	O(4)-Ho(1)-O(2)	99.4(3)
O(4)-Ho(1)-O(1W)	71.9(2)	O(1W)-Ho(1)-O(2)	76.7(3)
O(8)A-Ho(1)-O(7)	102.5(3)	O(7)-Ho(1)-O(2)	156.8(2)
O(4)-Ho(1)-O(7)	85.9(3)	O(2W)-Ho(1)-O(2)	127.6(2)
O(1W)-Ho(1)-O(7)	83.7(2)	O(8)A-Ho(1)-O(1)	79.8(3)
O(8)A-Ho(1)-O(2W)	72.4(3)	O(4)-Ho(1)-O(1)	76.9(3)
O(4)-Ho(1)-O(2W)	79.1(3)	O(1W)-Ho(1)-O(1)	115.0(3)
O(1W)-Ho(1)-O(2W)	145.2(2)	O(7)-Ho(1)-O(1)	148.2(3)
O(7)-Ho(1)-O(2W)	75.5(2)	O(2W)-Ho(1)-O(1)	75.1(2)
O(2)-Ho(1)-O(1)	54.2(2)	O(7)-Ho(1)-O(3W)	80.2(3)
O(8)A-Ho(1)-O(3W)	72.7(3)	O(2W)-Ho(1)-O(3W)	131.3(3)
O(4)-Ho(1)-O(3W)	140.5(3)	O(2)-Ho(1)-O(3W)	81.5(2)
O(1W)-Ho(1)-O(3W)	69.9(2)	O(1)-Ho(1)-O(3W)	129.3(3)

### 3

Sm(1)-O(4)	2.396(5)	Sm(1)-O(2)A	2.502(5)
Sm(1)-O(8)B	2.409(5)	Sm(1)-O(8)	2.512(5)
Sm(1)-O(5)B	2.414(5)	Sm(1)-O(7)	2.520(5)
Sm(1)-O(1)	2.450(5)	Sm(1)-O(1)A	2.548(5)
O(4)-Sm(1)-O(8)B	74.29(17)	O(4)-Sm(1)-O(8)	72.79(17)
O(4)-Sm(1)-O(5)B	138.10(16)	O(8)B-Sm(1)-O(8)	72.50(19)
O(8)B-Sm(1)-O(5)B	72.31(18)	O(5)B-Sm(1)-O(8)	73.58(16)
O(4)-Sm(1)-O(1W)	75.99(17)	O(1W)-Sm(1)-O(8)	121.02(17)
O(8)B-Sm(1)-O(1W)	141.09(18)	O(1)-Sm(1)-O(8)	104.73(16)
O(5)B-Sm(1)-O(1W)	144.31(18)	O(4)-Sm(1)-O(7)	74.70(19)
O(4)-Sm(1)-O(1)	142.05(18)	O(5)B-Sm(1)-O(7)	102.34(19)
O(5)B-Sm(1)-O(1)	71.16(17)	O(1W)-Sm(1)-O(7)	72.86(18)
O(1W)-Sm(1)-O(1)	73.49(18)	O(1)-Sm(1)-O(7)	75.15(16)
O(4)-Sm(1)-O(2)A	78.92(18)	O(2)A-Sm(1)-O(7)	143.66(19)
O(1W)-Sm(1)-O(2)A	76.8(2)	O(8)-Sm(1)-O(7)	51.30(15)
O(1)-Sm(1)-O(2)A	114.76(16)	O(8)B-Sm(1)-O(1)A	105.45(16)

### 4

Pr(1)B-O(1)	2.537(2)	Pr(1)A-O(5)	2.420(3)
Pr(1)-O(1)	2.594(2)	Pr(1)-O(7)	2.432(2)
Pr(1)-O(2)	2.542(3)	Pr(1)A-O(7)	2.621(2)
Pr(1)-O(4)	2.450(3)	Pr(1)A-O(8)	2.560(3)
Pr(1)-O(1W)	2.523(3)		
O(5)B-Pr(1)-O(7)	144.80(8)	O(1W)-Pr(1)-O(2)	74.07(9)
O(5)B-Pr(1)-O(4)	76.58(10)	O(5)B-Pr(1)-O(8)B	83.30(10)
O(7)-Pr(1)-O(4)	77.89(9)	O(7)-Pr(1)-O(8)B	102.57(8)
O(5)B-Pr(1)-O(1W)	141.09(9)	O(4)-Pr(1)-O(8)B	141.48(9)
O(7)-Pr(1)-O(1W)	71.87(8)	O(1W)-Pr(1)-O(8)B	72.64(9)
O(4)-Pr(1)-O(1W)	139.52(9)	O(1)A-Pr(1)-O(8)B	72.19(8)
O(5)B-Pr(1)-O(1)A	81.89(9)	O(2)-Pr(1)-O(8)B	145.29(9)
O(5)B-Pr(1)-O(2)	118.32(10)	O(7)-Pr(1)-O(1)	124.98(8)
O(7)-Pr(1)-O(2)	75.85(8)	O(4)-Pr(1)-O(1)	95.23(9)
O(4)-Pr(1)-O(2)	72.88(10)	O(1W)-Pr(1)-O(1)	81.18(9)
O(2)-Pr(1)-O(1)	50.60(8)	O(4)-Pr(1)-O(7)B	144.20(9)

### 5

Ce(1)-O(5)A	2.4546(16)	Ce(1)-O(1W)	2.5860(18)
Ce(1)-O(8)A	2.4775(17)	Ce(1)-O(4)	2.6303(17)
Ce(1)-O(1)B	2.4871(16)	Ce(1)-O(2W)	2.6459(18)
Ce(1)-O(7)	2.5150(16)	Ce(1)-O(5)	2.7563(17)
Ce(1)-O(2)	2.5857(17)	Ce(1)-O(1)	2.8146(17)
O(5)A-Ce(1)-O(8)A	70.98(6)	O(1W)-Ce(1)-O(4)	69.85(6)

O(8)A-Ce(1)-O(7)	129.25(5)	O(1)B-Ce(1)-O(2W)	81.13(6)
O(8)A-Ce(1)-O(2)	72.31(6)	O(7)-Ce(1)-O(2W)	65.57(6)
O(7)-Ce(1)-O(2)	138.25(6)	O(2)-Ce(1)-O(2W)	74.82(6)
O(5)A-Ce(1)-O(1W)	135.56(6)	O(1W)-Ce(1)-O(2W)	133.41(5)
O(8)A-Ce(1)-O(1W)	66.18(6)	O(4)-Ce(1)-O(2W)	137.67(6)
O(7)-Ce(1)-O(1W)	141.71(6)	O(1)B-Ce(1)-O(5)	114.68(5)
O(2)-Ce(1)-O(1W)	76.76(6)	O(7)-Ce(1)-O(5)	65.89(5)
O(5)A-Ce(1)-O(4)	117.45(6)	O(2)-Ce(1)-O(5)	134.57(5)
O(8)A-Ce(1)-O(4)	84.26(6)	O(1W)-Ce(1)-O(5)	102.52(5)
O(7)-Ce(1)-O(4)	76.88(6)	O(4)-Ce(1)-O(5)	47.86(5)
O(2)-Ce(1)-O(4)	144.86(6)	O(2W)-Ce(1)-O(5)	123.71(5)
O(8)A-Ce(1)-O(1)	110.62(5)	O(1W)-Ce(1)-O(1)	68.68(5)
O(7)-Ce(1)-O(1)	119.05(5)	O(4)-Ce(1)-O(1)	124.03(5)
O(2)-Ce(1)-O(1)	47.82(5)	O(2W)-Ce(1)-O(1)	64.83(5)
O(5)-Ce(1)-O(1)	170.78(5)		

Symmetry transformations used to generate equivalent atoms in **1**: **1**: A -x+1,-y,-z ; **2**: A -x+1,-y,-z ; **3**: A -x,-y+2,-z+1 ; B -x+1,-y+2,-z+1 ; **4**: A x,-y+1/2,z-1/2 ; B x,-y+1/2,z+1/2 ; **5**: A -x,-y,-z+1 ; B -x,-y+1,-z+1.

**Table 3.** Bond lengths (Å) and angles (°) of hydrogen-bond for **1-5**.

<i>D-H...A</i>	<i>d(D-H)</i>	<i>d(H...A)</i>	<i>d(D...A)</i>	$\angle DHA$
<b>1</b>				
O1W-H1WA...O2	0.96	1.89	2.797(10)	156
O3W-H3WA...O3	0.96	2.08	3.032(10)	169
O3W-H3WA...O2	0.96	2.58	3.200(11)	122

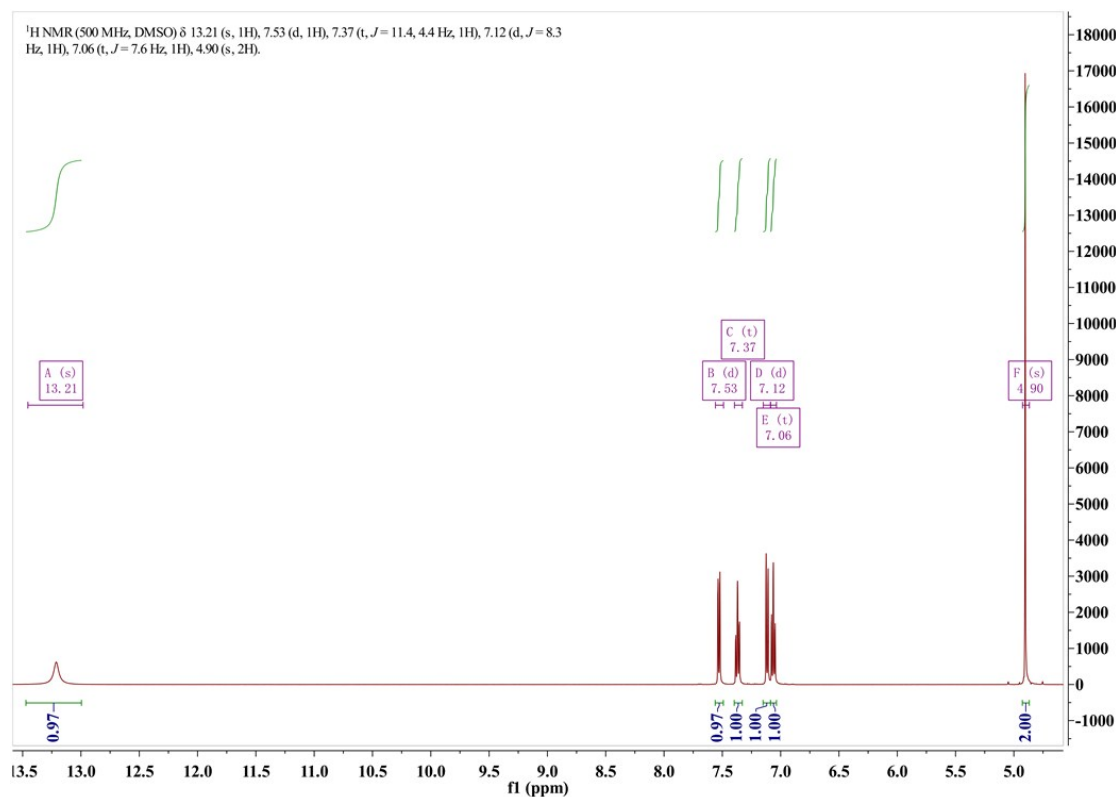


Fig. S5 <sup>1</sup>H NMR spectra of *o*-HCPA

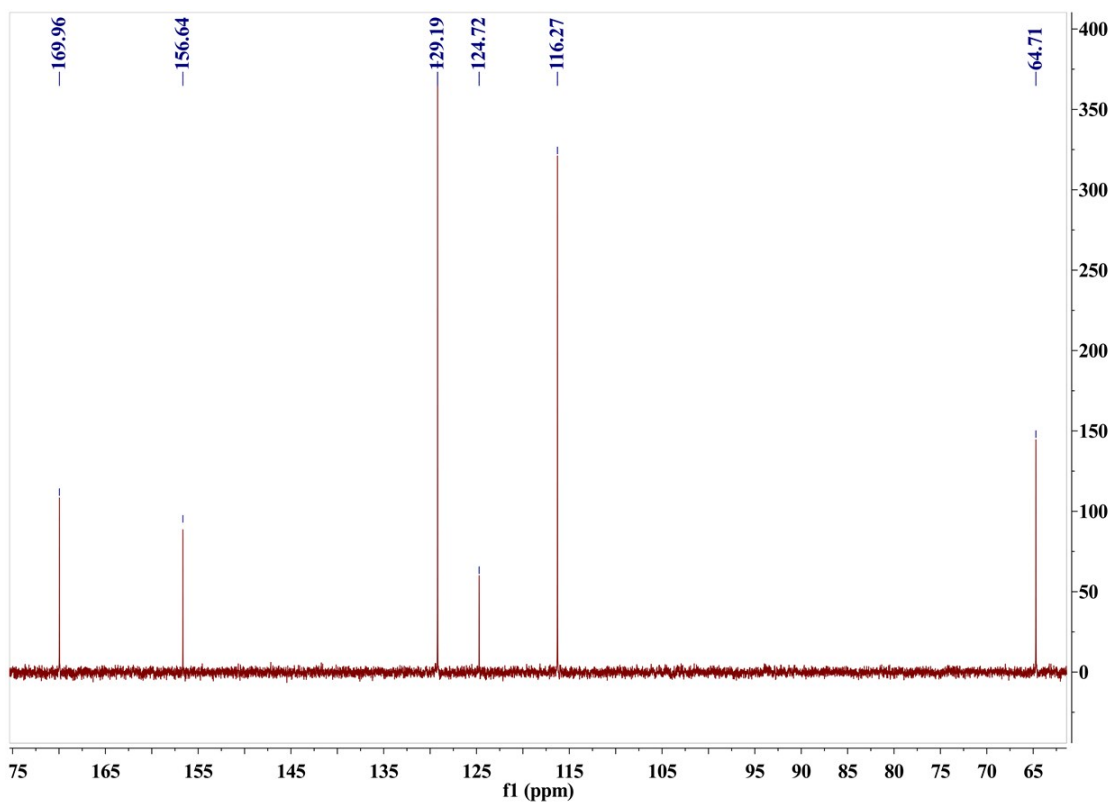


Fig. S6  $^{13}\text{C}$ NMR spectra of *o*-HCPA

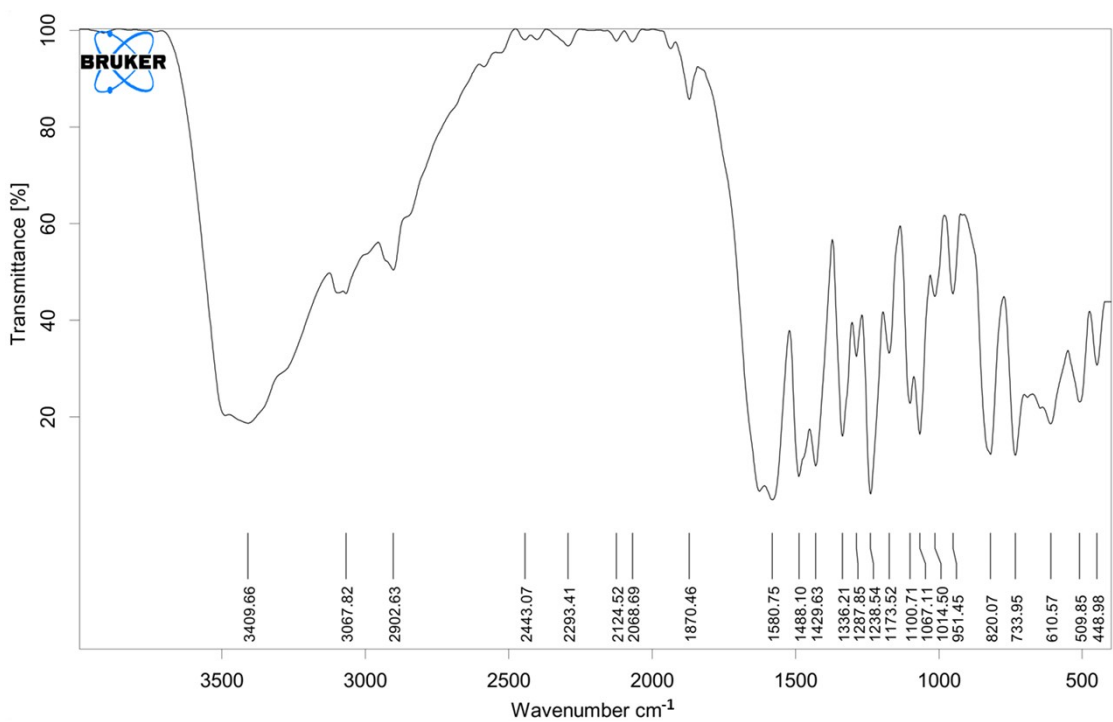


Fig. S7 IR spectra of compounds **1**.

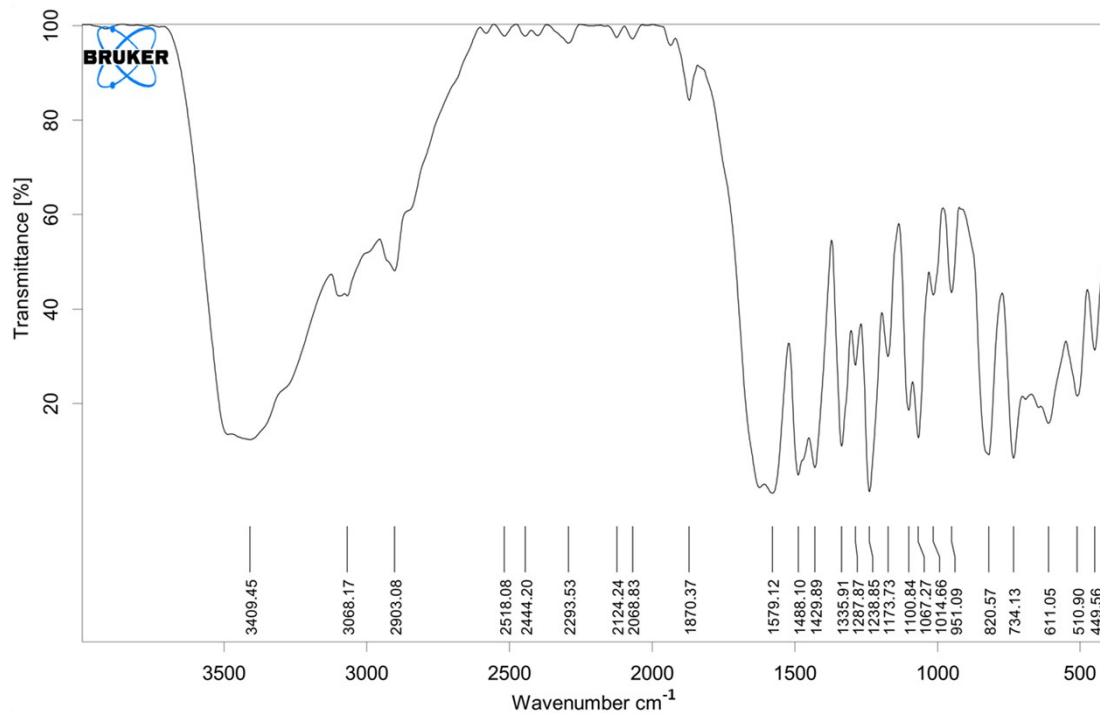


Fig. S8 IR spectra of compounds 2.

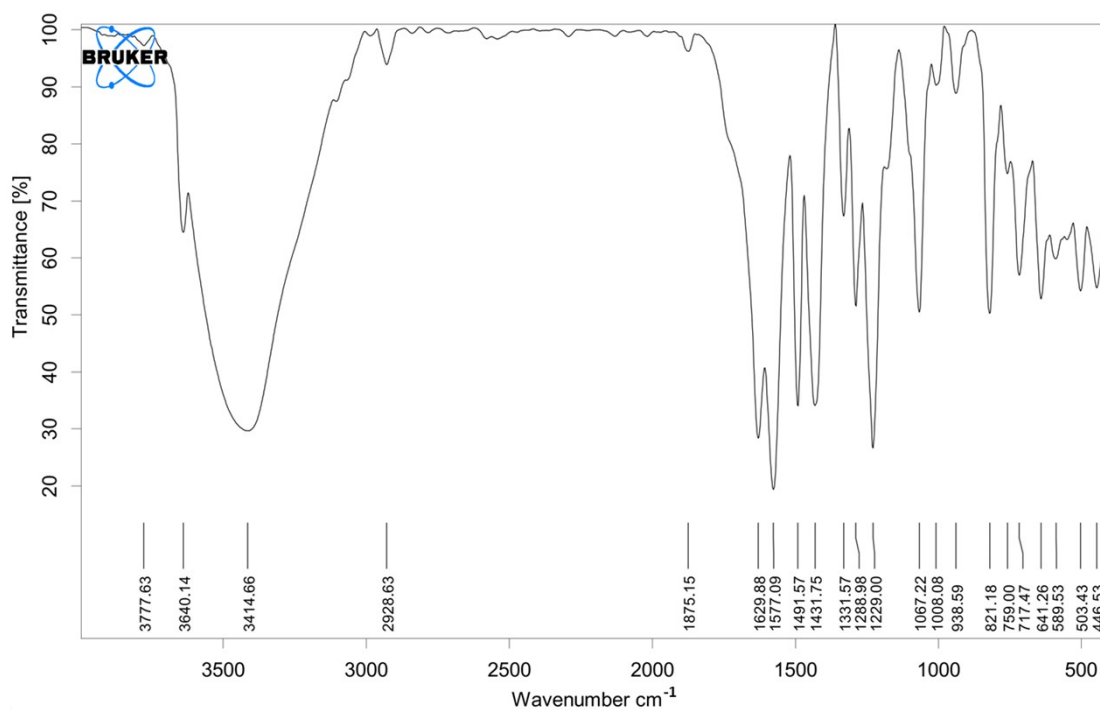


Fig. S9 IR spectra of compounds 3.

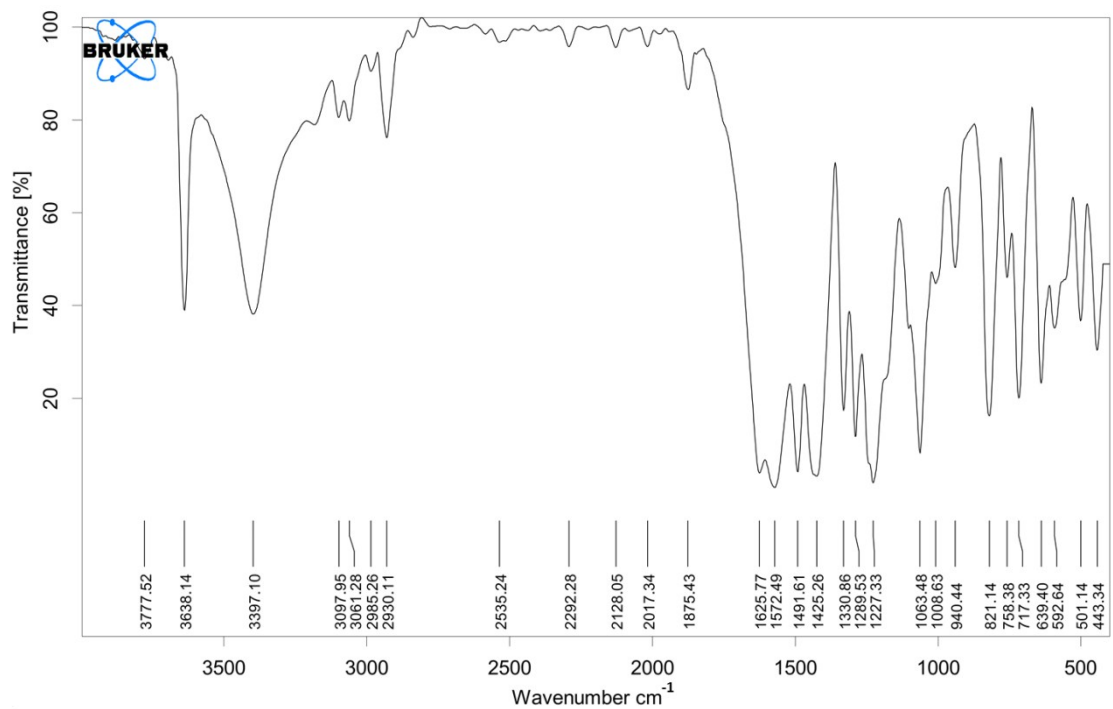


Fig. S10 IR spectra of compounds 4.

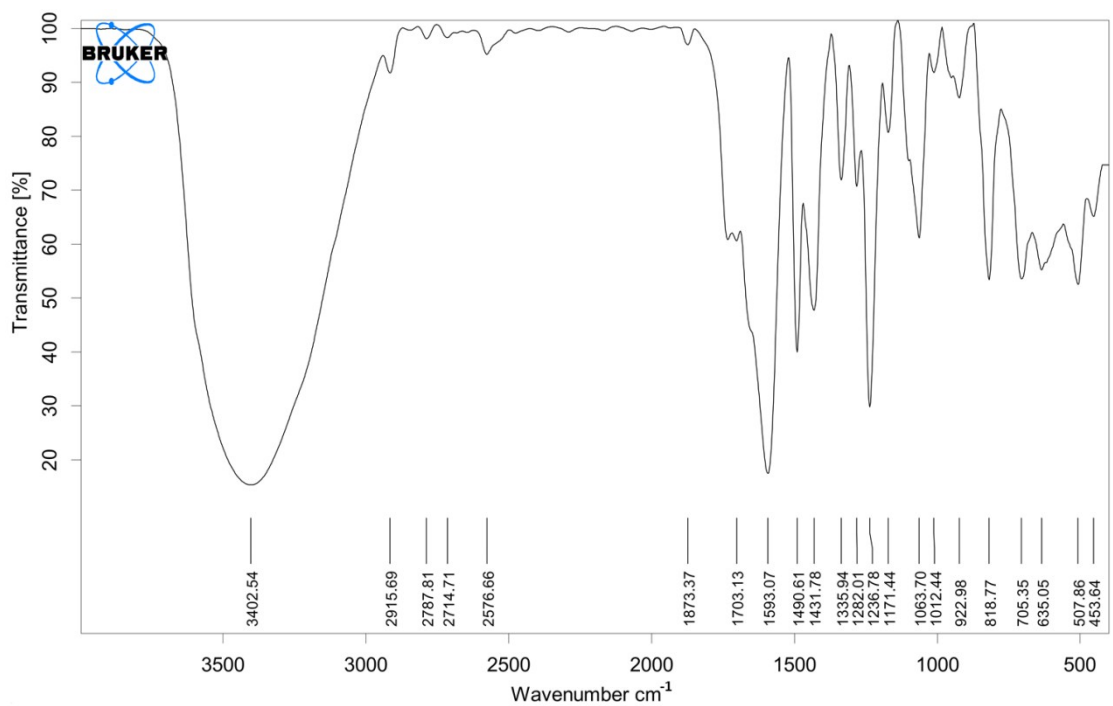


Fig. S11 IR spectra of compounds 5.